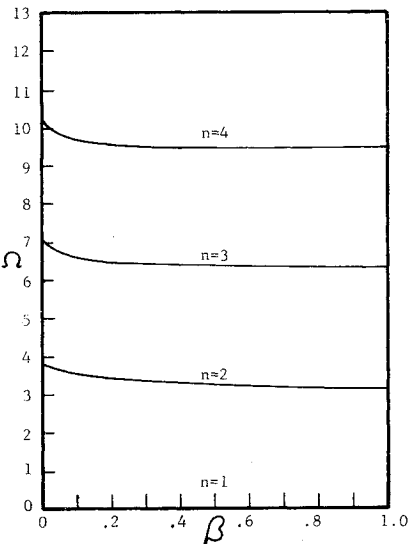


Fig. 4 Free-free case.



The values of Ω , as shown in Figs. 2-5 for $\beta = 1$, correspond exactly to those for circular bars with the same boundary conditions.

$\beta = 0$: The solutions for the free-fixed and free-free cases are determined as follows: Examination of Eq. (16) reveals that, in both cases, for a solution to exist, the constant D must equal zero; therefore, Eq. (17) can be rewritten as

$$(u_s)_{\beta=0} = C J_0(\omega S/a) e^{i\omega t} \quad (19)$$

$$(\epsilon_s)_{\beta=0} = -C J_1(\omega S/a) e^{i\omega t}$$

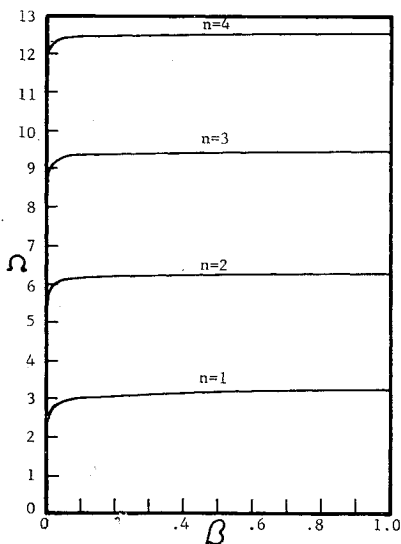
Substitution of the required boundary conditions yields, for the free-fixed case, $J_0(\Omega) = 0$ and, for the free-free case, $J_1(\Omega) = 0$. The limiting values of the frequency parameter Ω for the fixed-free and fixed-fixed cases are found from Eqs. (17): $J_1(\Omega) = 0$ for the fixed-free case and $J_0(\Omega) = 0$ for the fixed-fixed case.

Summary

The first four modes of the meridional vibrations in a conical shell of constant wall thickness have been determined for various cases of displacement boundary conditions.

The solution as presented is approximate in that the effects of lateral inertia are not included. Abramson, Plass, and Ripperger⁴ compare the exact solutions for axial wave propagation in rods of circular cross section with an approximate solution that does not include the effect of radial inertia. They conclude that the approximate solution is reasonably

Fig. 5 Fixed-fixed case.



accurate for pulses of very long duration, that is, where duration of the pulse is long compared with the time required for a wave front traveling at velocity a to move a distance equal to the diameter of the bar. If we apply an analogous line of reasoning to the cone problem, it would appear that the solution as presented is reasonably accurate if the ratio meridian length (pulse length) to wall thickness (bar diameter) is large. This condition should not be found overly restrictive in most engineering problems of practical interest.

References

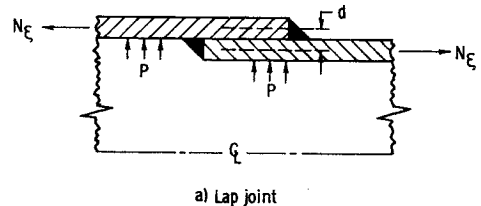
- ¹ Den Hartog, J. P., *Mechanical Vibrations* (McGraw-Hill Book Co., Inc., New York, 1956), p. 481.
- ² Timoshenko, S., *Theory of Plates and Shells* (McGraw-Hill Book Co., Inc., New York, 1940), Chap. X.
- ³ Pipes, L. A., *Applied Mathematics for Engineers and Physicist* (McGraw-Hill Book Co., Inc., New York, 1946), Chap. XIII.
- ⁴ Abramson, H. N., Plass, J. H., and Ripperger, E. A., "Stress wave propagation in waves and beams," *Advances in Applied Mechanics*, edited by H. L. Dryden and T. Von Karman (Academic Press Inc., New York, 1958), Vol. 4, pp. 113-138.

Mismatch Stresses in Pressure Vessels

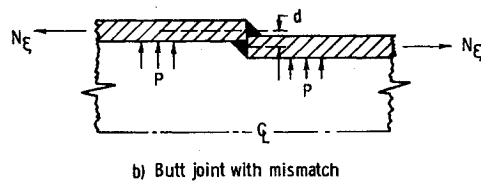
ROBERT H. JOHNS*

NASA Lewis Research Center, Cleveland, Ohio

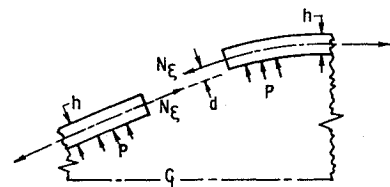
IN the manufacture of pressure vessels it is often necessary to join segments together at circumferential joints by welds or other means. Such connections may be made in lightweight flight tanks by lapping the segments and spot welding (Fig. 1a) or by butt welding the adjacent segments (Fig. 1b). The purpose of this note is to present an approximate analysis for the stresses arising at such a joint because of the mismatch or nonconcurrence of the middle surfaces of the adjoining segments which might occur. The method used is applicable to any nonshallow shell of revolution in which the meridional tangents of the two segments are parallel to each other at the junction.



a) Lap joint



b) Butt joint with mismatch



c) Joint with mismatch in general shell of revolution

Fig. 1 Mismatch joints and loading.

Received May 11, 1964; revision received June 29, 1964.

* Aerospace Engineer.

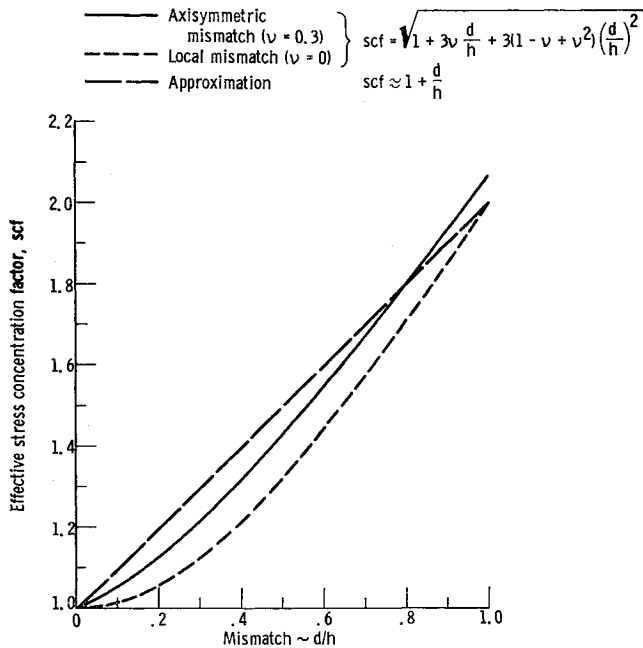


Fig. 2 Maximum effective stress due to mismatch in cylinder.

The methods presented offer the following advantages: 1) a simple closed-form solution is obtained which compares favorably with the results computed from linear edge-influence coefficients, 2) solutions are found which are applicable to both axisymmetric and local mismatches, and 3) an easily remembered approximate formula is suggested. The use of the equations presented herein avoids the necessity of using edge-loaded shell equations for the particular geometry being considered.

In Fig. 1, N_ξ is the meridional membrane force per unit length in the shells at their junction, and d is the distance between the middle surfaces (mismatch). Because of the eccentricity of the membrane forces, the bending moment at the junction is then

$$M_e = N_\xi d \quad (1)$$

If the shells are thin-walled and have equal thicknesses h , the eccentric moment will be distributed equally between the two shells. The maximum meridional stress occurs at the junction and is given by

$$\sigma_{\xi, \max} = \frac{N_\xi}{h} + \frac{6}{h^2} \frac{M_e}{2} \quad (2)$$

The maximum circumferential stress also occurs at the junction and, for nonshallow shells, is given by

$$\sigma_{\theta, \max} = \frac{N_\theta}{h} + \frac{6\nu}{h^2} \frac{M_e}{2} \quad (3)$$

where N_θ is the circumferential membrane force per unit length and ν is Poisson's ratio.

If the joint is a junction between two cylinders of radius a with internal pressure p , the foregoing equations can be written as

$$M_e = (pa/2)d \quad (1a)$$

$$\sigma_{\xi, \max} = (pa/2h)[1 + 3d/h] \quad (2a)$$

$$\sigma_{\theta, \max} = (pa/2h)[2 + 3\nu d/h] \quad (3a)$$

If the distortion-energy theory is used as a yield criterion, the maximum effective stress is

$$\sigma_e = (\sigma_\xi^2 + \sigma_\theta^2 - \sigma_\xi \sigma_\theta)^{1/2} \quad (4)$$

Substituting Eqs. (2a) and (3a) into (4) gives

$$\sigma_{e, \max} = \frac{3^{1/2}}{2} \frac{pa}{h} \left[1 + 3\nu \frac{d}{h} + 3(1 - \nu + \nu^2) \left(\frac{d}{h} \right)^2 \right]^{1/2} \quad (5)$$

for the case of mismatch in a cylinder of constant wall thickness. From Eq. (4) the effective stress in the membrane region of a pressurized thin cylinder $\sigma_{e, \text{mem}}$ can be shown to be $(3)^{1/2} pa/2h$. Therefore, the quantity in brackets in Eq. (5) can be considered a stress concentration factor due to the mismatch. Dividing Eq. (5) by $(3)^{1/2} pa/2h = \sigma_{e, \text{mem}}$ gives the stress concentration factor

$$scf = \frac{\sigma_{e, \max}}{\sigma_{e, \text{mem}}} = \left[1 + 3\nu \frac{d}{h} + 3(1 - \nu + \nu^2) \left(\frac{d}{h} \right)^2 \right]^{1/2} \quad (6)$$

Equation (6) is plotted in Fig. 2.

The results computed from the approximate analysis presented in Eq. (6) agree very favorably with the results computed from the linear edge influence coefficients described in Ref. 1; for example, the error was less than 2% for 100% mismatch and $a/h = 75$. The use of Eq. (6) precludes the necessity of determining edge influence coefficients and using the more rigorous equations indicated in Ref. 1. Contrary to the usual results obtained from edge influence coefficients, the stress concentration factor is independent of the cylinder radius.

In general, the mismatch would not be uniform around the circumference; however, if it is approximately constant for several characteristic lengths $(ah)^{1/2}$, the results should be sufficiently accurate for engineering purposes. If the mismatch is more of a local phenomenon, it might be more accurate to exclude the stresses due to the Poisson effect because the radial planes are no longer constrained to remain radial by axial symmetry, and local distortion can take place. Poisson strain due to bending is present, therefore, but not induced stress due to the Poisson effect. Consequently, for local mismatch let ν equal zero. Then

$$scf = \left[1 + 3 \left(\frac{d}{h} \right)^2 \right]^{1/2} \quad (7)$$

The result is identical to the one obtained from Ref. 2 if the overlap distance equals zero. Equation (7) is also plotted in Fig. 2. The radially symmetric case [Eq. (6)] can be considered an upper bound and is not much greater than the case for local mismatch if the mismatch is a relatively large percentage of the shell thickness.

If the junction between the two shells is a lap joint, additional discontinuity stresses arise because the increased thickness acts as a girdle, restricting expansion due to internal pressure. These additional stresses are not accounted for in this analysis. This effect may not be serious, however, because the restriction on the radial expansion tends to reduce the hoop stress, which is generally larger than the meridional stress. Thus, the stress concentration factor is probably reduced. Also, no effect of stress concentration due to sharp corners at the mismatch is included. If the joint is butt welded, there will probably be a fillet between the two sections which minimizes this effect.

One approximation of the effect of mismatch, which is easy to remember, is that the effective stress concentration factor is one plus the mismatch given as a fraction of the thickness. For example, if there is 50% mismatch, this approximation would give a stress concentration factor of 1.5. For axisymmetric or relatively wide mismatch, Eq. (6) gives 1.43 for the stress concentration factor. For relatively local mismatch, however, Eq. (7) gives 1.32. In Fig. 2, it is apparent that this simple approximation is reasonably accurate for large percentages of mismatch but is less accurate for small mismatch.

References

- Johns, R. H. and Orange, T. W., "Theoretical elastic stress distributions arising from discontinuities and edge loads in several shell-type structures," NASA TR R-103, Appendix L (1961).
- Sechler, E. E., "Stress rise due to offset welds in tension," Rept. EM 9-18, Space Technology Labs., Inc. (August 1959).